A Novel Methodology for Optimal Sizing Photovoltaic-Battery Systems in Smart Homes considering Grid Outages and Demand Response

Abstract –This paper deals with the optimal sizing of a hybrid photovoltaic-battery storage system for home energy management considering reliability against grid outages and demand response. To that end, a novel optimization framework is developed which aims at minimizing the electricity bill while the reliability of the system is ensured for certain common outages. In order to ensure the accuracy of the results, a large amount of characteristic outages along with demand, solar irradiance and temperature profiles are generated from real data. Clustering techniques are used for reducing this data to those most characteristics profiles and manage with the unpredictable behaviour of the outage events. Demand response is incorporated via different incentives like tariffs based on time of use and real time pricing, along with the optimal scheduling of different typical deferrable appliances. A case study on a smart- prosumer environment serves to illustrate the capabilities of the developed approach as providing sufficient guidelines for its universal applicability. Different cases studies are simulated considering different battery technologies and electricity tariffs for comparison. Various aspects related with the reliability against grid outages are also analysed like its impact on the project cost or the influence of demand response strategies.

***Keywords**:* Photovoltaic array, Battery storage, Home energy management, Reliability.

---

*Corresponding author, Tel.: +34 953 648518; Fax: +34 953 648586.
E-mail addresses: fjurado@ujaen.es (F. Jurado), mtostado@ujaen.es (M. Tostado-Véliz), dicazaa@ucacue.edu.ec (D. Icaza-Alvarez)

Acronyms

PV	Photovoltaic
BS	Battery storage
HEM	Home energy management
DR	Demand response
TOU	Time of use
RTP	Real time pricing
MILP	Mixed-Integer linear programming
PDF	Probability density function

Sets, Indexes and Functions

Ξ^{D}	Set of representative days
Ξ^{O}	Set of outage scenarios
Ω^{K}	Set of deferrable appliances
j	Index for years
s	Index for scenarios
t	Index for hours
k	Index for deferrable appliances
Ψ_s^{D}	Cluster of the representative day s
Ψ_s^{O}	Cluster of the outage scenario s
size$(\cdot)$	Yields the number of elements within a cluster

Parameters

T	Number of time intervals through a day
J	Number of years considered for the project
N	Number of generated outage scenarios
N^{R}	Number of representative days/outage scenarios (i.e. number of clusters)

57	N^{O}	Expected number of outage events per year
58	$\Delta\tau$	Time step (h)
59	r	Yearly inflation rate (pu)
60	ω_s	Weight of the representative scenario s
61	$\overline{Q^{\mathrm{BS}}}$	Maximum BS capacity allowed (kWh)
62	$\overline{P^{\mathrm{PV}}}$	Maximum rated power allowed for the PV array (kW)
63	$\overline{p^{\mathrm{BS}}}$	Rated power of the BS system (kW)
64	D^{BS}	Depth of discharge of the battery system (pu)
65	Q_0^{BS}	Initial state of charge of the BS system (kWh)
66	$\overline{p^{\mathrm{G}}}$	Maximum grid-to-home/home-to-grid power (kW)
67	$p_{s,t}^{\mathrm{ND}}$	Load demand attributable to non-deferrable appliances at representative scenario
68		s and time t (kW)
69	$\overline{p^k}$	Rated power of the deferrable appliance k (kW)
70	LB^k	Lower band of allowable operation time slot of the deferrable appliance k
71	UB^k	Upper band of allowable operation time slot of the deferrable appliance k
72	δ^k	Operation time slots of the deferrable appliance k
73	$i_{s,t}$	Solar irradiation at representative scenario s and time t (kW/m²)
74	$\theta_{s,t}$	Temperature at representative scenario s and time t (ºC)
75	η^{PV}	Efficiency of the PV array (pu)
76	$\eta^{\mathrm{BS,d}}$	Efficiency of the BS system (discharging) (pu)
77	$\eta^{\mathrm{BS,c}}$	Efficiency of the BS system (charging) (pu)
78	γ_j^{BS}	It is equal to 1 if the BS has to be replaced at year j (Binary)
79	γ_j^{PV}	It is equal to 1 if the PV array has to be replaced at year j (Binary)
80	κ^{PV}	Capital cost of the PV array ($/kW)

κ^{BS} Capital cost of the BS system ($/kWh)

μ^{PV} Operation and maintenance costs of the PV array ($/kW-yr)

μ^{BS} Operation and maintenance costs of the BS system ($/kWh-yr)

ν^{BS} Replacement cost of the BS system ($/kWh)

ν^{PV} Replacement cost of the PV array ($/kW)

$\lambda_{s,t}^{\mathrm{Tar}}$ TOU or RTP tariff at representative scenario s and time t ($/kWh)

$\lambda_{s,t}^{\mathrm{G,s}}$ Selling energy price at representative scenario s and time t ($/kWh)

$\mathbf{O}$ Matrix outage scenario. Its st^{th} element is equal to 0 if the utility grid is outage at representative scenario s and time t. Otherwise, this element would be equal to 1 (Binary)

$SP_{s,t}$ Instantaneous surplus power produced by the PV-BS system at representative scenario s and time t

Υ Budget limit ($)

Decision Variables

P^{PV} Rated power of the PV array (kW)

Q^{BS} Capacity of the BS system (kWh)

$p_{s,t}^{\mathrm{PV}}$ Power given by the PV array at representative scenario s and time t (kW)

$p_{s,t}^{\mathrm{BS,d}}$ Power delivered by the BS to the home at representative scenario s and time t (kW)

$p_{s,t}^{\mathrm{BS,c}}$ Power received by the BS from the home at representative scenario s and time t (kW)

$p_{s,t}^{\mathrm{G,b}}$ Grid-to-home power at representative scenario s and time t (kW)

$p_{s,t}^{\mathrm{G,s}}$ Home-to-grid power at representative scenario s and time t (kW)

$s_{s,t}$ Energy stored in the BS at representative scenario s and time t (kWh)

105 $u_{s,t}^{\mathrm{G,b}}$ It is equal to 1 if the utility grid is delivering power to the home at representative
106 scenario s and time t (Binary)
107 $u_{s,t}^{\mathrm{G,s}}$ It is equal to 1 if the utility grid is delivering power to the home at representative
108 scenario s and time t (Binary)
109 $u_{s,t}^{\sim}$ Commitment status of the appliances (Binary)
110 $\overline{u_{s,t}^{k}}$ It is equal to 1 if the deferrable appliance k is activated at representative scenario
111 s and time t (Binary)
112 $\underline{u_{s,t}^{k}}$ It is equal to 1 if the deferrable appliance k is deactivated at representative
113 scenario s and time t (Binary)

114 **1. Introduction**

115 Reliability of transmission grids is decreasing in some countries like U.S. [1]. Along
116 with this fact, climate change is driving an increasing number of large natural disaster
117 events [2]. These two issues are provoking that utility grid outages are becoming more
118 frequent nowadays [3]. Due to the significant socio-economic impact provoked by power
119 outages [4], the ability of networks and systems to face this kind of events with the
120 minimum damage has become a critical issue [5].

121 The ability of a power system to provide continuity supplying to the loads connected to
122 even under unforeseeable events is known in the literature as resilience or reliability.
123 Typically, the concept of resilience is used when a system is able to the ability to return
124 to a pre-disturbance condition when the disturbance is removed [6], and it is associated
125 to large extreme events; while reliability is rather considered for short-time low-impact
126 outages [2]. This paper is focused on the latter definition, it refers to reliability as the
127 ability of a system to provide continuity supplying to the loads connected to under short

time outage events. Nevertheless, we call the reader attention on the fact that both concepts, resilience and reliability, are frequently used indistinguishable.

There are multiple ways to achieve reliability and they mainly depend on the size and characteristics of the system or grid. Thus, reliability may be achieved by reconfiguring networks, deploying backup generators or promoting the usage of renewable sources and storage systems [2]. On the other hand, especially in small systems such as microgrids and nanogrids, demand response programs has achieved an important significance at planning stages of storage systems [7] or market-oriented tools [8]. Nevertheless, this kind of incentives and actions can be effectively coordinated [9] in order to reduce the impact of grid outages (e.g. see [10]).

At small-scale systems such as microgrids or dwellings, the overall usage of renewable-based generators and storage systems, along the promotion of DR programs, are the most conventional principles adopted for ensuring reliability against grid outages [11]. Storage systems are frequently deployed in combination with renewable generators such as PV arrays, in order to enable backup generation and demand response capacity to small-scale consumers. Thus, storage acts as backup generator and allows to effectively managing the energy generated by the PV array in order reduce the peak demand and alleviate the operation of the utility grid [12]. On the other hand, DR programs may encourage the users to modify their consumption patterns, so the operation of the utility grid can be alleviated and blackouts may be avoided [10].

Ensuring the reliability of end-users installations against utility grid contingencies supposes an effective way of guarantying the reliability of the whole system and reducing as much as possible their possible effects on people. In this context, the optimal planning of hybrid PV-BS systems considering DR programs becomes crucial to ensure system reliability at minimum cost. Despite this topic has been widely studied for distribution

grids (e.g. see [13]), no much works have been carried out at building-scale systems such as hospitals or dwellings.

D.P. Birnie III [14] presented a simple methodology to size a BS facility for a hybrid PV-BS system, so that it can work during grid outages. This reference is only focused on sizing the BS while the PV array is predefined. The real data at three localizations of U.S. is used in simulations. In this reference, it was assumed that all the energy produced by the PV system is stored in the BS, so that, considering two extreme events with limited sunlight and battery capacity, the capacity of the storage may be easily calculated by simply estimating the yearly sunlight hours.

The reference [15] analyzed the optimal operation of a BS system in a commercial building. The studied system encompasses a pre-sized PV array. The possibility of selling energy to the grid is also contemplated. The proposed scheduling model aims at enhancing the resilience of the system while the operation cost is kept at minimum level. This is achieved by including the conditional value at risk within the objective function.

In [16], a simulation-based tool for optimally sizing a BS system, which works coupling with a PV array in a hospital, is proposed. The proposed optimization framework incorporates some reliability-based indicators within the constraints of the problem and the loss of load as a penalty function within the objective function. Thus, the studied system is optimized for a predefined risk level. The simulation-based optimization framework used in this reference is carried out as follows. Firstly, the size of the PV array is set. Then, the capacity of the BS is varied within certain bounds and the objective function is calculated for each one. Thus, the pseudo-optimal size of the BS is determined.

The optimal designing of a PV-BS system for a rural remote area in Bolivia was tackled in [17]. Two loss of load scenarios are simulated by increasing the baseline demand of

three rural endings namely residential, school and health center. The sizing of the system is calculated by using genetic algorithms and only Li-ion batteries are considered.

E. Quiles et al. [18] proposed a novel methodology to determine the optimal size of a PV-BS system for supplying a local demand with reliability. This approach determines the size of the system from a deterministic point of view. Thus, the PV rated power equals to the peak load demand. Once the PV array is sized, a logical operating cycle between the PV and the BS is raised in order to determine the storage needs of the system. The stochastic demand and solar irradiance are simulated using the sequential Monte Carlo method and a series of stochastic outage events are randomly provoked some days of the year to calculate the capacity of the BS.

A hybrid system with PV array, Li-ion batteries and a backup diesel engine generator was optimally sized for a hospital in [19]. In this case, the resilience level of the system is determined through the tool ReOpt® [20]. The authors in [19] considered twelve scenarios: two extreme cases of solar irradiation, two outage starting times and three outage durations.

The authors find that the related state-of-art still present some gaps which are listed below:

- The optimal design of PV-BS systems at home-scale level is often carried out by simulation-based or deterministic approaches. Other references use metaheuristic techniques to size it. These approaches do not ensure the optimality of the results.
- Normally, the methodologies proposed are very rigid to adapt it to other scenarios and systems. In that sense, the possibility of DR or selling energy to the grid are relevant aspects, which would be difficulty studied by using the state-of-art approaches. In addition, the existing references do not normally consider DR and prosumer environments.

- To the best of our knowledge any related article has compared the results obtained for different DR incentives programs like tariffs based on TOU or RTP pricing; furthermore, only Li-ion batteries are customary contemplated. In addition, the existing approaches are not versatile enough to easily carry out this kind of comparative studies.

This work develops a novel methodology for comprehensive design of PV-BS system at home-scale level, which aims at overcoming the issues numerated above. The proposed approach is based on a home appliances scheduling model, which is raised as a MILP problem and solved analytically, ensuring the optimality of the results. In the concerned problem, DR programs are taken into account by incorporating different tariffs along with the optimal scheduling of some home appliances. Unlike to other methodologies, reliability of the utility grid is modelled via scenarios, which are generated from real data and incorporated to the optimization problem as constraints so that home demand has to be fully satisfied even in a presence of grid outage. The adopted approach has the following salient features:

- The uncertainty behavior of grid outages can be managed via scenarios. Thus, conventional techniques like Monte Carlo or clustering methods can be used to handle with.
- Outage events are characterized by PDFs, thus, as scenarios as required can be generated, in order to obtain reliable results.
- The generated outage events are generated based on real data. Therefore, the analyzed scenarios faithfully capture the idiosyncratic of each transmission/distribution system.

- The scenarios generated via the proposed approach are used here to size a PV-BS, however, as the procedure is very versatile, the same approach could be used to other systems and situations.

A case study on a smart prosumer environment is analyzed in order to illustrate the capabilities of the developed approach. However, the applicability of the developed methodology is not only limited to the case study showed in this paper. In order to extend the scope of this research to other situations, sufficient guidelines to the universal applicability of the proposed approach are provided.

The remainder of this paper is organized as follows. Section 2 outlines the home system under study. The methodology employed in this work for optimally design a PV-BS system is explained in Section 3. Section 4 presents the mathematical formulation of the developed optimal appliances scheduling problem. Section 5 presents and comments various numerical results. Finally, the main conclusions are duly drawn in Section 6.

2. The home system under study

Fig. 1 pictorially represents the home system under study. This system is supplied through a utility grid and encompasses a PV-BS facility along a set of deferrable and non-deferrable loads. Three typical deferrable appliances have been considered in this article and their main characteristics are summarized in Table 1 [21]. As seen, the sequential operation constraint of some appliances is guaranteed by imposing operating time windows. Such is the case of the spin dryer, which cannot be operated until the wasing machine has completed its operating cycle. It is assumed that the home utility is governed by a HEM system which can schedule the operation of the deferrable appliances (within predefined time windows) and the PV-BS system on the basis of pricing signals; while the non-deferrable loads are operated on the basis of users decisions and, consequently,

249 they cannot be controlled by the HEM tool. The analysed system can either buy or sell
250 energy from/to a utility grid for convenience.

251 This research is focused on grid outages. During a blackout event, it is assumed the
252 total unavailability of the grid, therefore, energy cannot flow between the home and the
253 utility grid. On the face of this situation, the supplying of the home system must be
254 ensured by own resources which in our case encompasses a PV-BS system. Also, the
255 home system could not sell energy to the grid during an outage event.

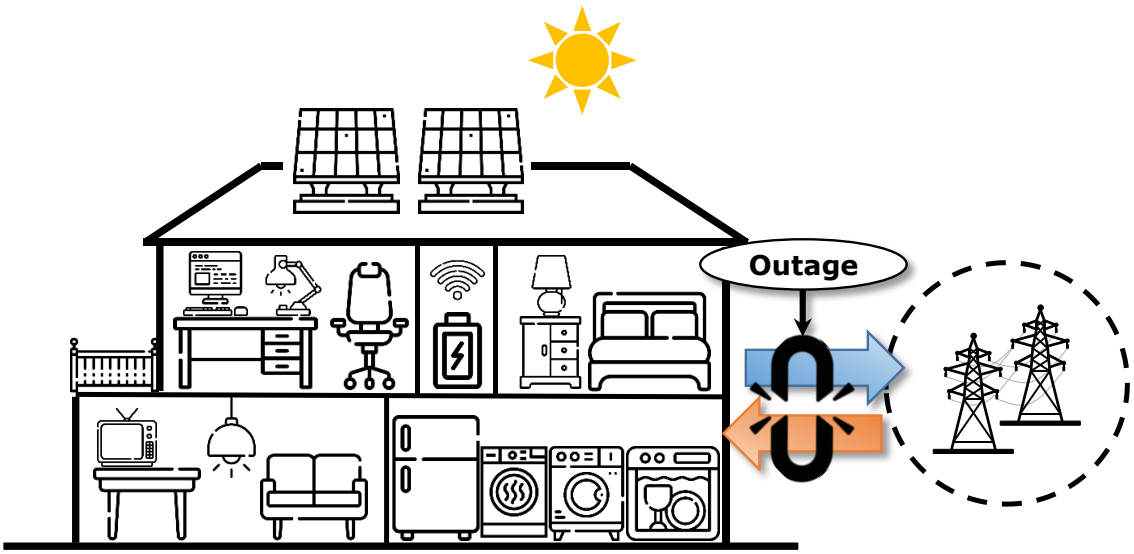

256
257 Fig. 1. Pictorial representation of the home system under study

258 Table 1. Main characteristics of the deferrable appliances [21]

Appliance (k)	$\overline{p^k}$ **(kW)**	LB^k	UB^k	δ^k
Washing machine	3	16	23	3
Dishwasher	2.5	15	33	4
Spin dryer	2.5	25	35	2

259

260 ## 3. Methodology

261 The following sections describe the proposed methodology for optimal sizing a PV-BS
262 facility for a home system taking into consideration DR incentives and reliability. The
263 different unpredictable variables brought by PV availability, load demand, etc., have been
264 modelled, as customary, via scenarios [22].

265 ### 3.1. *Grid outage events characterization*

In this paper, we propose to model a series of characteristic short-time outages so that the instantaneous demand has to be fully satisfied any moment even in the presence of utility grid failure. In this case, each outage event is characterized by its starting time and duration, which can be considered random variables. In order to manage with random variables and reproduce accurate results, a huge amount of outage events are generated based on historical data. With the aim at generating a huge amount of outage scenarios, it is proposed to model the available outage data as PDFs. Then, by using the the inverse transform method [23], as scenarios as required can be generated from the constructed PDFs.

Conventional techniques to manage with random variables, such as the Monte Carlo method [23], require to handle a huge amount of scenarios in order to capture the random behavior of the concerned variable. The amount of data generated is often quite large and difficulty tractable in practice. In order to easily manageable this data without compromising the accuracy of the results, it is proposed to cluster the different scenarios in order to only consider the most characteristic events. Clustering techniques are devoted on modelling a set of raw data by only some characteristic members. Among the plethora of clustering techniques available in the literature, the aggregation methods can be considered the most popular ones for optimally planning energy systems [24]. Among the different aggregation techniques available in the literature, the k-medoids method has been used in this work due to it is frequently considered as the most reliable [25]. The k-medoids method presents a degree of freedom namely the total number of clusters generated. For our case, each cluster corresponds with an outage event which is considered in simulations. This way, the total number of clusters (i.e. outage events) taken influences the accuracy of the results obtained. On the other hand, if many clusters are considered, the optimization method may entail an unaffordable computational burden.

Therefore, the total number of clusters should be selected as a trade-off solution between accuracy and efficiency. In order to determine the most suitable number of clusters for the considered problem, one can observe the value of some support indicators like the Davies-Bouldin index [26]. Fig. 2 summarizes the proposed methodology to generate outage events based on real data.

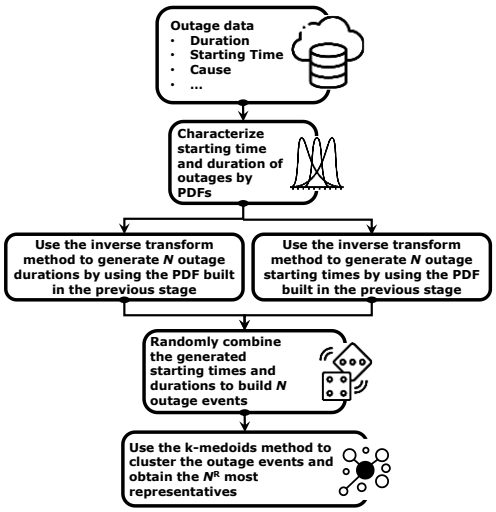

Fig. 2. Flowchart of the proposed methodology to generate characteristic grid outage events

3.2. *Representative days*

In order to keep the coherency through the developed methodology, the other stochastic variables involved in the problem (i.e. non-deferrable appliances demand, solar irradiation and temperature) have been modelled in a similar way to the outage events. This way, it is assumed that measured data of these variables is available. Thus, the available measurements are temporally representing by means of characteristic days by using the k-medoids method. Fig. 3 summarizes the procedure adopted for characterizing the non-deferrable appliances demand, solar irradiation and temperature as representative days.

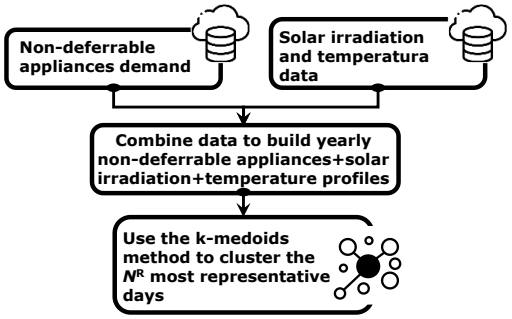

Fig. 3. Flowchart of the proposed procedure for characterizing the non-deferrable appliances demand, solar irradiation and temperature based on real data

3.3. *Proposed optimal PV-BS sizing approach*

In real life, very few days through a year are expected to experience outage events. Therefore, the developed approach calculates the size of the PV-BS system considering two conditions: with and without consideration of grid outages. In this regard, two kind of scenarios are taken into account. The scenarios without grid outages are simply simulated taking the representative days constructed in Section 3.2, considering that the utility grid is available any moment. On the other hand, the scenarios with consideration of grid outages (namely 'outage scenarios'), are built by randomly combined the representative days obtained in the Section 3.2 with the outage events generated in the Section 3.1. Thus, the characteristic outage events are simulated through the different representative days. These scenarios serve as input of a developed MILP optimal PV-BS sizing problem which is further described in Section 4. Fig. 4 schematically summarizes the methodology adopted for optimally design a PV-BS system with consideration of grid outages and DR incentives.

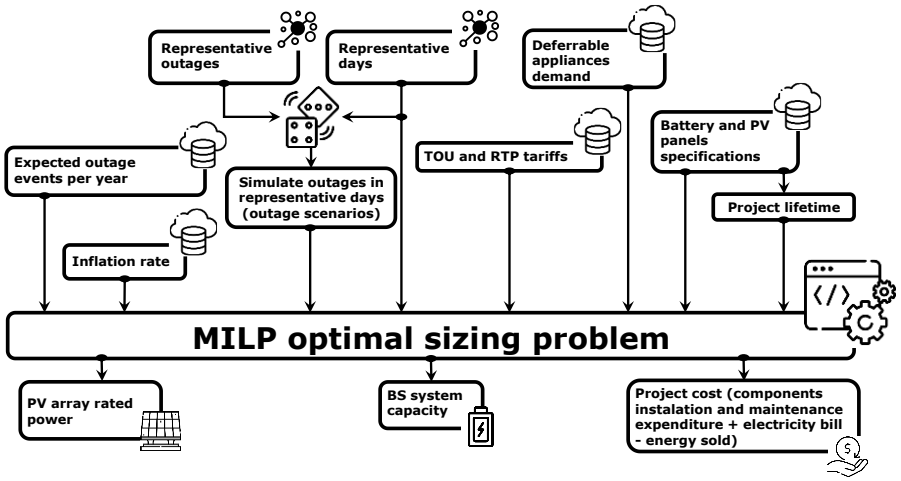

Fig. 4. Flowchart of the proposed methodology for optimal sizing a PV-BS system.

4. Mathematical Formulation of the optimal PV-BS sizing problem

4.1. *Objective Function*

The objective function aims at minimizing the total PV-BS cost through the project lifetime as follows:

$$\min_{\boldsymbol{x}} \underbrace{Q^{\mathrm{BS}}\kappa^{\mathrm{BS}} + P^{\mathrm{PV}}\kappa^{\mathrm{PV}}}_{Capital\ costs} + \sum_{j=1}^{j=J}(1 + r)^{(j-1)} \left\{ \underbrace{Q^{\mathrm{BS}}\left(\gamma_j^{\mathrm{BS}}\nu^{\mathrm{BS}} + \mu^{\mathrm{BS}}\right) + P^{\mathrm{PV}}\left(\gamma_j^{\mathrm{PV}}\nu^{\mathrm{PV}} + \mu^{\mathrm{PV}}\right)}_{Yearly\ costs} + \sum_{s=1}^{s=N^{\mathrm{R}}} \omega_s \left[\sum_{t=1}^{t=T} \Delta\tau \left(\underbrace{\lambda_{s,t}^{\mathrm{Tar}} p_{s,t}^{\mathrm{G,b}} - \lambda_{s,t}^{\mathrm{G,s}} p_{s,t}^{\mathrm{G,s}}}_{Daily\ costs} \right) \right] \right\} \quad (1)$$

where $\boldsymbol{x}$ is the vector of decision variables (see *'Decision Variables'* in Nomenclature section). As seen, the function (1) encompasses a series of different costs which are evaluated over different time horizons. Firstly, the project incurs in capital costs once during its lifetime. Secondly, expenditures corresponding with replacement and fixed maintenance costs are considered once each year during the project lifetime. The binary variables $\gamma_j^{\sim}$ force to the replacement costs to be only considered when the equipment have passed their expected lifetime. Finally, the daily costs are related with the energy exchanged between the home system and the utility grid.

The different considered scenarios are weighted when they are taken into account in (1). These weights aim at representing how many days through a year can be straightforward represented by each representative day. Hence, for those scenarios without consideration of grid outages, the different weights are given by:

$$\omega_s = \text{size}(\Psi_s^{\text{D}});\ \forall s \in \Xi^{\text{D}} \tag{2}$$

On the other hand, only few days are expected to experience grid outages through a year. In fact, the expected number of outages in U.S. during 2018 was estimated to be 1.3 events per year [27]. Therefore, the different outage scenarios should be weighted in (1) accordingly. If the expected number of outages per year is equal to N^{O}, the weight of each outage scenario can be calculated as follows:

$$\omega_s = \frac{N^{\text{O}}}{N^{\text{R}}}\text{size}(\Psi_s^{\text{O}});\ \forall s \in \Xi^{\text{O}} \tag{3}$$

Intuitively, N^{O} representative days should not be considered in (2) in order to keep (1) coherent (i.e. $\sum_{\forall s \in \Xi^{\text{D}}} \text{size}(\Psi_s^{\text{D}}) + \sum_{\forall s \in \Xi^{\text{O}}} \frac{N^{\text{O}}}{N^{\text{R}}} \text{size}(\Psi_s^{\text{O}}) = 365$). In this case, N^{O} days are subtracted from that cluster with the largest number of elements within it.

4.2. *Constraints*

4.2.1. *Utility Grid*

The instantaneous power that can flow from/to the utility grid to/from the home system is upper bounded as modelled the equations (4) and (5). Also, both purchasing and selling energy processes are complementary as indicated the equation (6).

$$0 \leq p_{s,t}^{\text{G,b}} \leq u_{s,t}^{\text{G,b}} \overline{p^{\text{G}}};\ \forall t \in T, \forall s \in \Xi^{\text{D}} \cup \Xi^{\text{O}} \tag{4}$$

$$0 \leq p_{s,t}^{\text{G,s}} \leq u_{s,t}^{\text{G,s}} \overline{p^{\text{G}}};\ \forall t \in T, \forall s \in \Xi^{\text{D}} \cup \Xi^{\text{O}} \tag{5}$$

$$u_{s,t}^{\text{G,b}} + u_{s,t}^{\text{G,s}} \leq 1;\ \forall t \in T, \forall s \in \Xi^{\text{D}} \cup \Xi^{\text{O}} \tag{6}$$

During a grid outage, the energy cannot flow from/to the utility grid. This constraint is modelled by the equations (7) and (8). As seen, if a grid outage takes place at time t and scenario s, the value of the matrix event takes zero. Therefore, by constraints (7) and (8), the binary variables $u_{s,t}^{\mathrm{G,b}}$ and $u_{s,t}^{\mathrm{G,s}}$ are forced to be zero as well. This way, by constraints (4) and (5), the power that flows from/to the utility grid is forced to be zero, which emulates the unavailability of the utility grid.

$$u_{s,t}^{\mathrm{G,b}} \leq \mathbf{O}(s,t);\ \forall t \in T, \forall s \in \Xi^{\mathrm{O}} \tag{7}$$

$$u_{s,t}^{\mathrm{G,s}} \leq \mathbf{O}(s,t);\ \forall t \in T, \forall s \in \Xi^{\mathrm{O}} \tag{8}$$

4.2.2. *PV Array*

The instantaneous power given by the PV array depends on the availability of solar irradiance and ambient temperature. Furthermore, it can be calculated as follows [28]:

$$p_{s,t}^{\mathrm{PV}} = P^{PV} i_{s,t}\left\{0.8 + 0.024\left(\theta_{s,t} + i_{s,t}[33.8 - 37.5\eta^{PV}] - 25\right)\right\} = P^{PV}\phi_{s,t};\ \forall t \in T, \forall s \in \Xi^{\mathrm{D}} \cup \Xi^{\mathrm{O}} \tag{9}$$

In practise, the value of $\phi_{s,t}$ should not be much larger than 1, since it would mean that the PV array can supply more power than its nominal value. In this work, it is considered that overloads up to 10% over the nominal power are allowed, therefore, the value of $\phi_{s,t}$ will be always upper bounded to 1.10. Although the instantaneous power given by the PV array is fixed by (9), the inverter can set it lower if required. Thus, the following constraint must be satisfied.

$$0 \leq p_{s,t}^{\mathrm{PV}} \leq P^{PV}\phi_{s,t};\ \forall t \in T, \forall s \in \Xi^{\mathrm{D}} \cup \Xi^{\mathrm{O}} \tag{10}$$

At home level, the rated power of the PV array is also conditioned by surround factors, as for instance the surface available to install PV panels or the monetary budget available for the users. For those reasons, the capacity of the PV system will be upper bounded in order to avoid that the optimization problem yields unrealistic results:

$$P^{PV} \leq \overline{P^{\mathrm{PV}}} \tag{11}$$

4.2.3. *BS System*

The power given by the batteries is upper bounded by equipment limits, as modelled the equations (12) and (13). The charging and discharging processes must be complementary, as forced by the equation (14). The equation (15) represents the state of charge of the BS system, which is upper and lower bounded by its capacity and depth of discharge as indicated the constraint (16). The equations (17) and (18) denote the initial and final state of charge of the BS system.

$$0 \leq p_{s,t}^{\mathrm{BS,d}} \leq u_{s,t}^{\mathrm{BS,d}} \overline{p^{\mathrm{BS}}};\ \forall t \in T, \forall s \in \Xi^{\mathrm{D}} \cup \Xi^{\mathrm{O}} \tag{12}$$

$$0 \leq p_{s,t}^{\mathrm{BS,c}} \leq u_{s,t}^{\mathrm{BS,c}} \overline{p^{\mathrm{BS}}};\ \forall t \in T, \forall s \in \Xi^{\mathrm{D}} \cup \Xi^{\mathrm{O}} \tag{13}$$

$$u_{s,t}^{\mathrm{BS,d}} + u_{s,t}^{\mathrm{BS,c}} \leq 1;\ \forall t \in T, \forall s \in \Xi^{\mathrm{D}} \cup \Xi^{\mathrm{O}} \tag{14}$$

$$s_{s,t} = s_{s,t-1} + \Delta\tau \left(\eta^{\mathrm{BS,c}} p_{s,t}^{\mathrm{BS,c}} - \frac{p_{s,t}^{\mathrm{BS,d}}}{\eta^{\mathrm{BS,d}}} \right);\ \forall t \in T \backslash t > 1, \forall s \in \Xi^{\mathrm{D}} \cup \Xi^{\mathrm{O}} \tag{15}$$

$$Q^{\mathrm{BS}}(1 - D^{\mathrm{BS}}) \leq s_{s,t} \leq Q^{\mathrm{BS}};\ \forall t \in T, \forall s \in \Xi^{\mathrm{D}} \cup \Xi^{\mathrm{O}} \tag{16}$$

$$s_{s,1} = Q_0^{\mathrm{BS}}; \forall s \in \Xi^{\mathrm{D}} \cup \Xi^{\mathrm{O}} \tag{17}$$

$$s_{s,T} = Q_0^{\mathrm{BS}}; \forall s \in \Xi^{\mathrm{D}} \cup \Xi^{\mathrm{O}} \tag{18}$$

As in the case of the PV array, the capacity of the BS system will be upper limited as follows:

$$Q^{\mathrm{BS}} \leq \overline{Q^{\mathrm{BS}}} \tag{19}$$

4.2.4. *Deferrable Appliances*

The deferrable appliances should meet various requirements. Firstly, the deferrable appliances have to be scheduled once each day even in the presence of grid outages. This requirement is satisfied by the equation (20). The deferrable appliances have to be operated continuously, this behaviour is modelled by the equation (21). Finally, the

deferrable appliances have to complete their operating cycles within their allowable time windows, as forced by the equation (22).

$$\sum_{t=1}^{t=T} \overline{u_{s,t}^{k}} = 1;\ \forall k \in \Omega^{\mathrm{K}}, \forall s \in \Xi^{\mathrm{D}} \cup \Xi^{\mathrm{O}} \tag{20}$$

$$\overline{u_{s,t}^{k}} - \underline{u_{s,t}^{k}} = u_{s,t}^{k} - u_{s,t-1}^{k};\ \forall t \in T \backslash t > 1, \forall k \in \Omega^{\mathrm{K}}, \forall s \in \Xi^{\mathrm{D}} \cup \Xi^{\mathrm{O}} \tag{21}$$

$$\sum_{t=LB^{k}}^{t=UB^{k}} u_{s,t}^{k} = \delta^{k}; \forall k \in \Omega^{\mathrm{K}}, \forall s \in \Xi^{\mathrm{D}} \cup \Xi^{\mathrm{O}} \tag{22}$$

4.2.5. *Budget Limit*

Planning tools in smart homes are strongly influenced by limitations on the monetary expenditures that the users are willing to undertake. In order to reflect this restriction in the considered problem, the constraint (23) is added.

$$Q^{\mathrm{BS}} \kappa^{\mathrm{BS}} + P^{\mathrm{PV}} \kappa^{\mathrm{PV}} \leq \Upsilon \tag{23}$$

Equation (23) forces that the total initial capital costs of the project cannot be higher than a predefined budget limit (Υ).

4.2.6. *System Balance*

In the developed model, reliability is achieved by ensuring that the home demand is fully satisfied even in the presence of short-time grid outages. It is assumed that the HEM system can freely schedule the deferrable appliances along the operation of the PV-BS in order to meet this requirement. Therefore, the constraint (24) must be fully satisfied any moment.

$$p_{s,t}^{\mathrm{G,b}} + p_{s,t}^{\mathrm{PV}} + p_{s,t}^{\mathrm{BS,d}} = p_{s,t}^{\mathrm{G,s}} + p_{s,t}^{\mathrm{BS,c}} + p_{s,t}^{\mathrm{ND}} + \sum_{\forall k \in \Omega^{\mathrm{K}}} u_{s,t}^{k}\, \overline{p^{k}};\ \forall t \in T, \forall s \in \Xi^{\mathrm{D}} \cup \Xi^{\mathrm{O}} \tag{24}$$

Power losses due to energy transportation are not modelled in (24) due to two reasons:

- Active power losses are marginal in home systems and are customary neglected [21].

- Power consumption attributable to the non-deferrable loads is assumed to be obtained from metering data, which typically includes the power losses.

Nevertheless, energy losses can be easily incorporated by simply adding an estimation of them in the right side of (24).

5. Case study

This section presents an application of the developed methodology on a prosumer environment. The selected case study responds to the model developed in Section 4, which aims at being generic enough to sufficiently describe the capabilities of the developed method as providing proper guidelines to apply the developed approach to any other home system and situation. The benchmark prosumer environment considered in this work corresponds with that described in Fig. 1 and mathematically modelled in Section 4. The results presented in this section have been obtained by carrying out the MILP model described in Section 4, following the flowchart of Fig. 4. The mathematical formulation of the considered optimization problem was coded and solved in Matlab R2019a.

5.1. *Data*

Real information about the major grid outages occurred in U.S. in the period 2000-2016 has been considered. This information is freely available from [29] and it has been previously taken in [30]. Two main characteristic of each outage are on interest for the present study: its duration and starting time. Fig. 5 represents the available data in form of histograms. As seen, most of analysed outages had a very short duration (< 1 min).

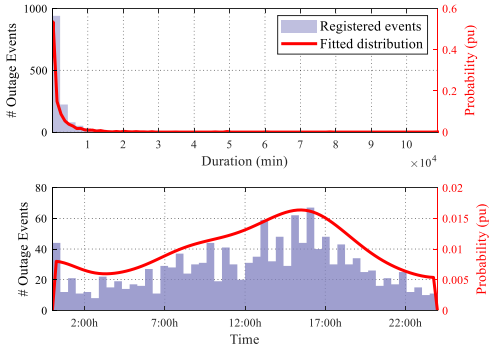

Fig. 5. Data available for major grid outages occurred in U.S. during the period 2000-2016. Top figure shows the histogram and the fitted kernel distribution (red line) for the outage durations, while the same is showed at bottom for the outage starting time.

The historic data collected in [29] has to be modelled as PDFs in order to generated scenarios based on it. As suggested in [30], kernel PDFs have been selected for characterizing the both concerned variables. Fig. 5 plots with red lines the fitted PDFs according to the available data. These distributions have been built by using kernel normal estimators for 100 equally-spaced points on both random variables. Using the fitted PDFs, up to $N = 10{,}000$ scenarios have been generated. In this case, as this paper is focused on short time events, those outages longer than 240 minutes have been neglected, assuming that longer events should be covered by grid resources home-level facilities are supposed to have a limited capacity. This way, the total considered scenarios has been reduced to approximately $N = 5{,}500$ in our case.

As commented, the data generated is quite large and difficulty tractable in practice. In this work, it is proposed to use the k-medoids technique in order to reduce it without compromising the accuracy of the results obtained. As mentioned, the total number of clusters (i.e. outage events) to generate can be selected on the basis of some helpful indexes. For this case study, two popular indicators namely the total sum of distances (which is the total sum of the distances among each medoid with respect to the members of its cluster) and the Davies Bouldin index [26] have been used. Intuitively, the lower

value of each index, the better clustering number. However, the lowest value of the both indexes is not typically obtained for the same clustering number. Therefore, a compromise solution should be normally adopted. For the case study, Fig. 6 plots the value of the two considered metrics for the grid outage events registered in [29]. As seen, the lowest Davies-Bouldin value was observed with 3 clusters, however, the total sum of distances was unacceptable in this case. Furthermore, $N^{\mathrm{R}} = 15$ seems a suitable choosing. Finally, the characteristic grid outage events constructed by using the proposed methodology are pictorially represented in Fig. 7.

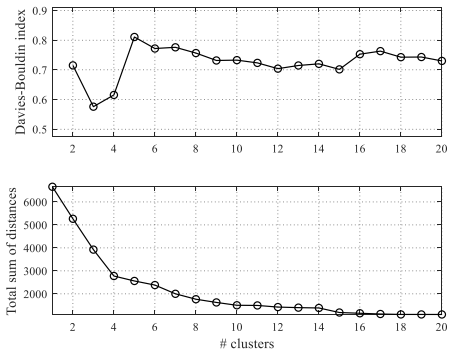

Fig. 6. Value of the metrics used for evaluating different clustering numbers for grid outage events

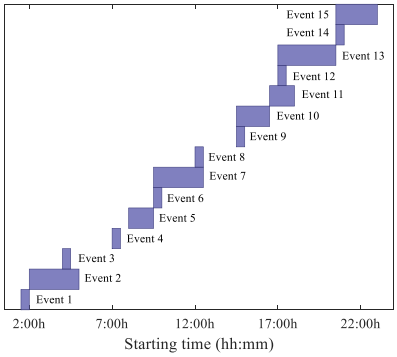

Fig. 7. Characteristic grid outage events generated by the proposed methodology

The non-deferrable appliances demand has been taken from [31], which corresponds with real-data measured on a smart home through a year. The considered raw data is especially suitable as it includes the total losses occurred in the system, which avoids the necessity of modelling them. The available data is adapted to 30-min resolution by simply considering the average load during the period. Solar irradiation and temperature data

with 1-h resolution is provided by the European Comssion for the year 2016. In this case, solar irradiation and ambient temperature collected for Los Angeles (U.S.) has been used. The 15 representative days taken for simulations are shown in Fig. 8.

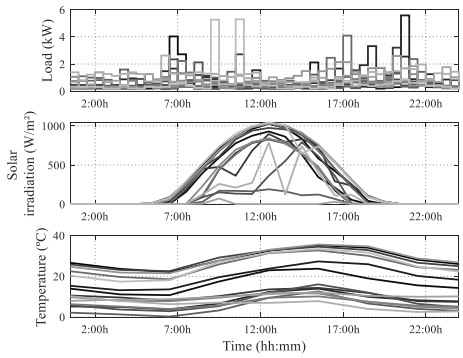

Fig. 8. Representative days taken for non-deferrable appliances demand (top), solar irradiation (middle) and ambient temperature (bottom)

A pessimist scenario has been considered which up to 2 grid outages are expected through a year. The inflation rate has been taken equal to 1.26%. The TOU and RTP tariffs are showed in Fig. 9 and have been extracted from the reference [21]. The selling prices have been considered 0.9 times the purchasing prices in both tariffs. The specifications of the PV array and BS system are reported in Tables 2 and 3 [32, 33], and. Lead-Acid and Li-ion battery technologies have been considered for this study. The project lifetime has been considered 25 years. The data of the deferrable appliances is collected in Table 1. Lastly, the values $\overline{p^{\mathrm{BS}}} = 3\mathrm{kW}$, $\overline{p^{\mathrm{G}}} = 10\mathrm{kW}$, $Q_0^{\mathrm{BS}} = Q^{\mathrm{BS}}$, $\eta^{PV} = 0.13$, $\overline{P^{\mathrm{PV}}} = 4\mathrm{kW}$, $\overline{Q^{\mathrm{BS}}} = 10\mathrm{kWh}$ and $\Upsilon = 7{,}500\ \$$ have been taken.

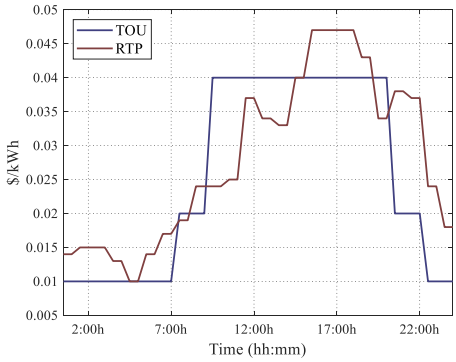

Fig. 9. TOU and RTP tariffs considered in simulations

Table 2. Specifications of the PV array

Capital cost	1,210 $/kW
Maintenance cost	15 $/kW-yr
Replacement cost	484 $/kW
Expected lifetime	25 yrs

Table 3. Specifications of the BS system

	Lead-Acid	Li-ion
Capital cost	300 $/kWh	300 $/kWh
Maintenance cost	3.75 $/kWh-yr	2.75 $/kWh-yr
Replacement cost	240 $/kWh	300 $/kWh
Expected lifetime	6 yrs	12 yrs
D^{BS}	0.60	0.60
$\eta^{\mathrm{BS,d}}/\eta^{\mathrm{BS,c}}$	0.70	0.98

Two cases are studied. Firstly, it is considered that the grid is available any hour through the year, therefore, the outage scenarios are not considered in the optimization problem. On the other hand, a series of characteristic outages are considered in order to simulate blackout events of the utility grid (outage scenarios). These scenarios take part jointly with the representative days.

5.2. *Results considering total availability of the utility grid*

Table 4 reports the most relevant results obtained for two cases study: with and without the installation of the PV-BS system. As expected, the designed optimization problem determined that the installation of a storage system is not beneficious in this case since the utility grid is fully reliable. As seen, notably monetary savings may be achieved by installing a PV array. More precisely, the installation of a PV array allows to reduce the monetary expenditures up to 4,200 $ and 3,467 $ with TOU and RTP tariff, respectively.

Table 4 – Main results obtained without considering grid outages

Case			Objective function ($)	P^{PV} (kW)	Q^{BS} (kWh)
Without PV-BS	TOU		6,945	--	--
	RTP		7,367	--	--
With PV-BS	TOU	Lead-Acid	2,745	4	0
		Li-ion	2,745	4	0
	RTP	Lead-Acid	4,300	4	0
		Li-ion	4,300	4	0

The usage of a PV array allowed to reduce the monetary bill of the users in two ways. On the one hand, it allows to the smart home to be self-sufficient at hours with high PV potential. On the other hand, in some cases a surplus energy can be generated, which can be sold to the grid in order to obtain a monetary revenue. These two processes are clearly illustrated in Fig. 10, where the scheduling result of the PV array along the total appliances (deferrable and non-deferrable) are showed for a representative day with Li-ion batteries. As seen, during the central hours, the total home demand is fully covered by the PV array. During this period, a surplus energy (gray shaded area) can be produced by the PV array, which is entirely destined to be sold to the grid.

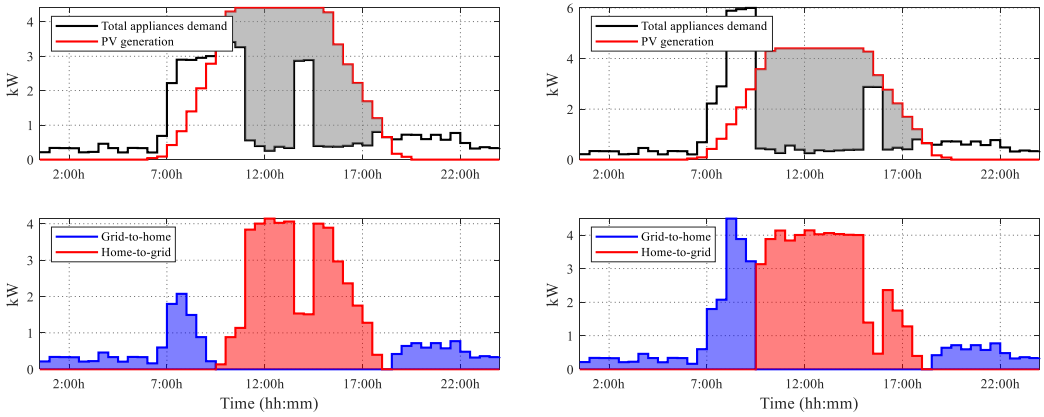

Fig. 10. PV scheduling result for a typical day without grid outages with RTP (left) and TOU tariff (right)

The deferrable appliances were scheduled so the monetary bill is reduced. This is clearly appreciated in Fig. 11, where the scheduling results for the deferrable appliances at the same day showed in Fig. 10 are displayed. In this figure, the instantaneous surplus power has been calculated as follows:

$$SP_{s,t} = \max\left(0, p_{s,t}^{\mathrm{PV}} - p_{s,t}^{\mathrm{ND}}\right);\ \forall t \in T, \forall s \in \Xi^{\mathrm{D}} \tag{25}$$

The value of (25) gives an idea of when the home can be partially or totally supplied by own resources and, consequently, the energy cost is zero. This will be true only when the demand attributable to the non-deferrable loads does not surpasses the value yielded

by (25). Indirectly, this expression illustrates the most favorable periods to schedule the non-deferrable loads. As seen in Fig. 11, in the case of RTP tariff, both the washing machine and the spin dyer are scheduled within time slots where their operation is favorable. On the other hand, the dishwasher was scheduled at 7:30 h, when its rated power was higher than the total surplus power. It means that this load was partially supplied by the PV array, however, certain amount of energy had to be purchased from the grid in order to satisfy this demand. This was done so because if this device is scheduled later, the total demand attributable to non-deferrable loads would surpass the total surplus power. This had forced to the home to acquire energy to the grid at those hours when the energy is very expensive. For the case with TOU tariff, one can observe that both the washing machine and dishwasher were partially supplied by the grid. In this case, this option was preferable since at 9:00 h the TOU tariff is abruptly increased (see Fig. 9). In this regard, it is more profitable to sell the surplus energy to the grid rather than devoted it to supply the washing machine and dishwasher at central hours of the day, when the surplus energy is high. Thus, these appliances were scheduled at hours with very low energy price while the surplus energy was entirely dedicated to obtain monetary revenues.

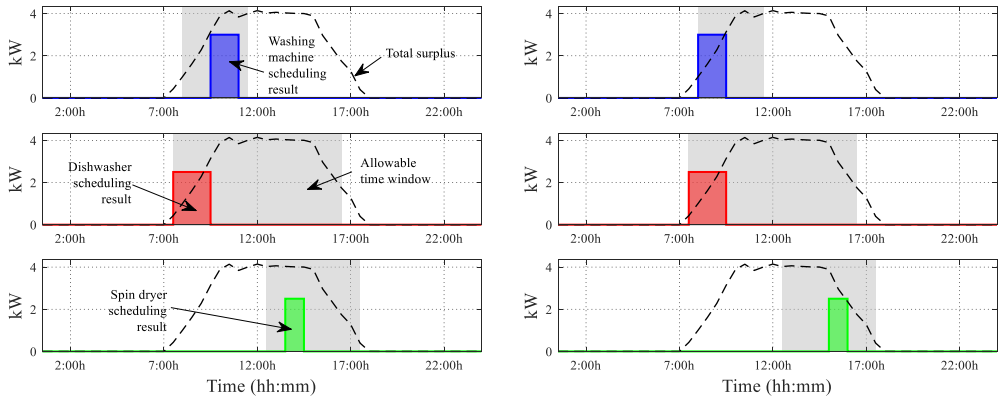

Fig. 11. Deferrable appliances scheduling result for a typical day without grid outages with RTP (left) and TOU tariff (right)

5.3. *Results in the presence of grid outages*

570 Table 5 is analogue to Table 5 for the case in which grid outage scenarios are considered
571 in the problem. In this case, results without PV-BS were not calculated since the
572 constraint (24) can be only satisfied by deploying a PV-BS system. As seen, storage
573 facilities have to be installed in order to ensure the reliability of the home system during
574 grid blackouts. As observed, if one compares the results of this table with those reported
575 in Table 4 for the case with PV-BS system, including reliability requirements increased
576 the project cost up to 9,226 $.

577 Table 5. Main results obtained considering grid outages

Case		Objective function ($)	P^{PV} (kW)	Q^{BS} (kWh)
TOU	Lead-Acid	11,732	4	8.3
	Li-ion	7,217	4	8
RTP	Lead-Acid	13,526	4	8.3
	Li-ion	8,835	4	8

578

579 Fig. 12 displays the PV-BS scheduling result for a typical day with Li-ion batteries. In
580 this case, the utility grid was out of service during three hours (9:30 h – 12:30 h). As seen,
581 during outage, the home demand is partially covered by the PV array or the BS system,
582 depending on the availability of solar irradiation. The BS system also allows to reduce
583 the dependency to the utility grid, as seen, during expensive hours (evening-night), the
584 BS facility tends to be discharged in order to fully or partially cover the home demand,
585 while the energy is recovered during last hours of the day, when the energy price is falling
586 down.

587

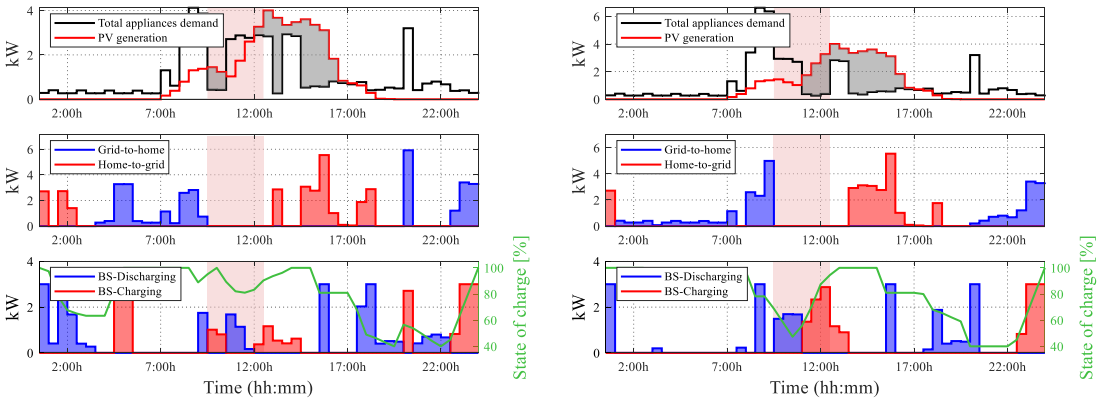

Fig. 12. PV-BS scheduling result for a typical day with grid outage (denoted by red shaded area) considering Li-ion batteries with RTP (left) and TOU tariff (right)

Fig. 13 is analogue to Fig. 11 for the day represented in Fig. 12. Here, the instantaneous surplus power is given by:

$$SP_{s,t} = \max\left(0, p_{s,t}^{\mathrm{PV}} + p_{s,t}^{\mathrm{BS,d}} - p_{s,t}^{\mathrm{ND}} - p_{s,t}^{\mathrm{BS,c}}\right);\ \forall t \in T, \forall s \in \Xi^{\mathrm{D}} \cup \Xi^{\mathrm{O}} \tag{26}$$

Similar scheduling results were obtained with both tariffs. As observed, the different deferrable appliances are operated out of outage periods. This was done so since, otherwise, these appliances had to be partially supplied by the BS system. This fact had undoubtedly forced to oversize the storage system, incurring in large capital and maintenance costs.

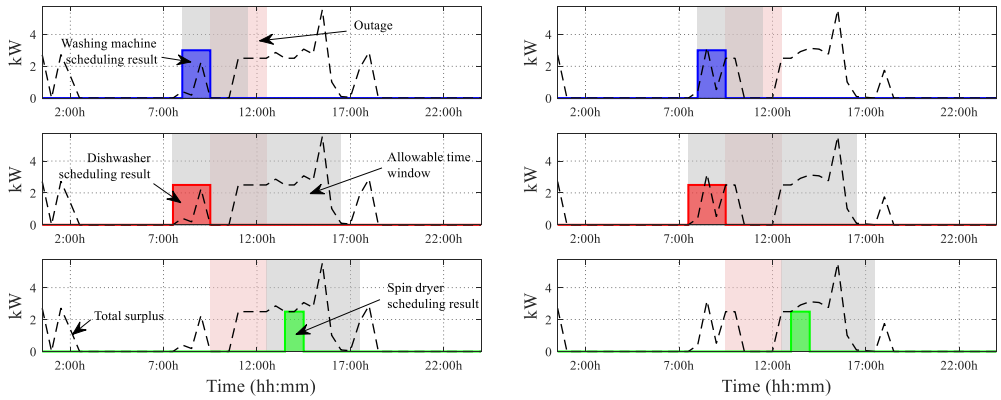

Fig. 13. Deferrable appliances scheduling result for a typical day with grid outage (denoted by red shaded area) with RTP (left) and TOU tariff (right)

5.4. *Regarding the universal applicability of the developed methodology*

In this research, results have been reported for just a case study, since covering all possible casuistry results unaffordable in this case. For that reason, the applicability of

605 the developed method to other home systems and outage events deserves a further
606 explanation, which is provided in this section.

607 The case study corresponds to a benchmark prosumer environment. This case aimed at
608 being sufficiently generic to describe a wide range of potential situations that may take
609 place in real life. Nevertheless, the developed methodology is versatile enough to easily
610 accommodate a large number of different scenarios. The developed methodology requires
611 very usual data, which are commonly encountered on public database or metering on-site
612 by using smart infrastructures. The MILP optimization model can be also adapted to other
613 potential situations. For example, different renewable-based sources and deferrable
614 appliances can be accommodated as is described in Section 4, it would be just necessary
615 to incorporate as variables and constraints as devices or loads are contemplated. Also, as
616 the prosumer environment is a special case of the consumer one, the latter situation can
617 be perfectly derived from that described in Section 4. Such a case, it is just necessary to
618 remove the variables and constraints related with the variables associated to the power
619 flow from the home system to the utility grid.

620 On the other hand, this paper is only focused on grid outages. However, similar
621 approach can be considered for simulating and analyzing the failure of other devices such
622 as the PV-BS system. For example, if one desires to analyses the behavior of the home
623 system under BS failure events, one can create a BS matrix failure such as $\mathbf{O}^{\mathrm{BS}}(s,t)$. This
624 new matrix would work in a similar way to that used in the constraints (7) and (8), This
625 way, $\mathbf{O}^{\mathrm{BS}}(s,t)$ would be equal to 0 if the BS system is unavailable at time t and scenario
626 s and equal to 1 otherwise. Also, a pair of constraints similar to (7) and (8) but related to
627 $u_{s,t}^{\mathrm{BS,c}}$ and $u_{s,t}^{\mathrm{BS,d}}$ (i.e. $u_{s,t}^{\mathrm{BS,c}} \leq \mathbf{O}^{\mathrm{BS}}(s,t)$; $u_{s,t}^{\mathrm{BS,d}} \leq \mathbf{O}^{\mathrm{BS}}(s,t)$) should be added to the MILP
628 problem described in Section 4, in order to emulate the BS system failure.

629 5.5. *Computational burden*

It is worth remarking the computational burden of the whole developed methodology as its possible main barrier to be used in larger or more complex systems. In that sense, the resolution of the developed MILP model described in Section 4 supposes the main bottleneck of the developed methodology, assuming that the other stages can be carried out in an efficient way on conventional software. In this regard, for our particular case, the whole methodology was carried out in approximately 10 minutes for each case study on an average machine (64-bit i5-8500F Intel Core personal computer (3 GHz, 8 GB of RAM)), which is acceptable for this kind of tools. However, the computational burden of MILP problems grows with their complexity (number of variables), which may limit the usage of the developed methodology on other larger systems. On the face of this situation, advanced software facilities like Gurobi [34] and parallel processing strategies can be implemented to alleviate the computational effort. Nevertheless, it is worth mentioning that the developed approach is devoted on planning stages. In such cases, computational time is not as important as in operating conditions [32].

6. Conclusions and Future Works

A novel methodology for optimally sizing a home PV-BS system considering grid outages and DR incentives has been presented. In the developed approach, the grid outages are considered via characteristic scenarios which are modelled in the optimization problem as constraints, while the DR is taken into account by properly modelling the scheduling of deferrable appliances and considering different tariffs like TOU and RTP programs. The resulting optimization problem is a MILP, which can be straightforward solved on average machines using conventional software.

A case study on a smart prosumer environment has been analysed to show the capabilities of the developed methodology and providing sufficient guidelines for its universal applicability. Two scenarios with and without considering grid failures have

been carried out in order to show how the developed approach is able to effectively size a PV-BS system taking into account reliability and DR programs along as evaluating the monetary cost of ensuring reliability at end-users level.

Ongoing works are conducted on developing novel online control algorithms for the home system proposed here, taking into account possible grid outages jointly with DR incentives.

7. Acknowledgments

The icons used in the figures of this article were made by Freepik from www.flaticon.com.

8. References

[1] N.D. Laws, K. Anderson, N.A. DiOrio, X. Li, J. McLaren, Impacts of valuing resilience on cost-optimal PV and storage systems for commercial buildings, Renew. Energy 127 (2018) 896-909. https://doi.org/10.1016/j.renene.2018.05.011

[2] M. Panteli, P. Mancarella, Influence of extreme weather and climate change on the resilience of power systems: Impacts and possible mitigation strategies, Electr. Power Syst. Res. 127 (2015) 259-270. https://doi.org/10.1016/j.epsr.2015.06.012

[3] A. Hussain, V.-H. Bui, H.-M. Kim, Microgrids as a resilience resource and strategies used by microgrids for enhancing resilience, Appl. Energy 240 (2019) 56-72. https://doi.org/10.1016/j.apenergy.2019.02.055

[4] A. Gholami, F. Aminifar, M. Shahidehpour, Front Lines Against the Darkness: Enhancing the Resilience of the Electricity Grid Through Microgrid Facilities, IEEE Electrific. Mag. 4(1) (2016) 18-24. https://doi.org/10.1109/MELE.2015.2509879

[5] H. Gao, Y. Chen, Y. Xu, C. Liu, Resilience-Oriented Critical Load Restoration Using Microgrids in Distribution Systems, IEEE Trans. Smart Grid 7(6) (2016) 2837-2848. https://doi.org/10.1109/TSG.2016.2550625

[6] T.J. Overbye, Engineering resilient cyber-physical systems, in: 2012 IEEE Power and Energy Society General Meeting, San Diego, CA; 2012, pp. 1-1. https://doi.org/10.1109/PESGM.2012.6344943

[7] M.S. Javadi, A. Anvari-Moghaddam, J.M. Guerrero, Optimal Planning and Operation of Hybrid Energy System Supplemented by Storage Devices, in: 7th International Solar Integration Workshop, Berlin; 2017

[8] R. Sharifi, A. Anvari-Moghaddam, J.M. Guerrero, V. Vahidinasab, An optimal market-oriented demand response model for price-responsive residential consumers, Energy Efficiency 12 (2019) 803-815. https://doi.org/10.1007/s12053-018-9713-x

[9] A. Anvari-Moghaddam, G. Mokhtari, J.M. Guerrero, Coordinated Demand Response and Distributed Generation Management in Residential Smart Microgrids, in: L. Mihet-Popa (Eds.), Energy Management of Distributed Generation Systems, InTech Europe, 2016. https://doi.org/10.5772/63379

[10] M. Vahedipour-Dahraie, H. Rashidizadeh-Kermani, A. Anvari-Moghaddam, Risk-Based Stochastic Scheduling of Resilient Microgrids Considering Demand Response Programs, IEEE Syst. J. 2020 (Early Access). https://doi.org/ 10.1109/JSYST.2020.3026142

[11] T. Khalili, A. Jafari, M. Abapour, B. Mohammadi-Ivatloo, Optimal battery technology selection and incentive-based demand response program utilization for reliability improvement of an insular microgrid, Energy 169 (2019) 92-104. https://doi.org/10.1016/j.energy.2018.12.024

[12] F. Shariatzadeh, P. Mandal, A.K. Srivastava, Demand response for sustainable energy systems: A review, application and implementation strategy, Renew. Sustain. Energy Rev. 45 (2015) 343-350. https://doi.org/10.1016/j.rser.2015.01.062

[13] J. Dong, F. Gao, X. Guan, Q. Zhai, J. Wu, Storage-Reserve Sizing With Qualified Reliability for Connected High Renewable Penetration Micro-Grid, IEEE Trans. Sustain. Energy 7(2) (2016) 732-743. https://doi.org/10.1109/TSTE.2015.2498599

[14] D.P. Birnie III, Optimal battery sizing for storm-resilient photovoltaic power island systems, Sol. Energy 109 (2014) 165-173. https://doi.org/10.1016/j.solener.2014.08.016

[15] M. Tavakoli, F. Shokridehaki, M.F. Akorede, M. Marzband, I. Vechiu, E. Pouresmaeil, CVaR-based energy management scheme for optimal resilience and operational cost in commercial building microgrids, Int. J. Elect. Power Energy Syst. 100 (2018) 1-9. https://doi.org/10.1016/j.ijepes.2018.02.022

[16] S. Tsianikas, J. Zhou, D.P. Birnie III, D.W. Coit, Economic trends and comparisons for optimizing grid-outage resilient photovoltaic and battery systems, Appl. Energy 256 (2019) 113892. https://doi.org/10.1016/j.apenergy.2019.113892

[17] F. Benavente, A. Lundblad, P.E. Campana, Y. Zhang, S. Cabrera, G. Lindbergh, Photovoltaic/battery system sizing for rural electrification in Bolivia: Considering the suppressed demand effect, Appl. Energy 235 (2019) 519-528. https://doi.org/10.1016/j.apenergy.2018.10.084

[18] E. Quiles, C. Roldán-Blay, G. Escrivá-Escrivá, C. Roldán-Porta, Accurate Sizing of Residential Stand-Alone Photovoltaic Systems Considering System Reliability, Sustainability 12(3) (2020) 1274. https://doi.org/10.3390/su12031274

[19] A. Lagrange, M. de Simón-Martín, A. González-Martínez, S. Bracco, E. Rosales-Asensio, Sustainable microgrids with energy storage as a means to increase power resilience in critical facilities: An application to a hospital, Int. J. Elect. Power Energy Syst. 119 (2020) 105865. https://doi.org/10.1016/j.ijepes.2020.105865

[20] NREL. Renewable Energy Integration & Optimization, https://reopt.nrel.gov/tool. Denver: National Renewable Energy Laboratory, 2018 (accessed 8 January 2021).

[21] M.S. Javadi, M. Gough, M. Lotfi, A.E. Nezhad, S.F. Santos, J.P.S. Catalão, Optimal self-scheduling of home energy management system in the presence of photovoltaic power generation and batteries, Energy 210 (2020) 118568.

[22] B. Zhao, A.J. Conejo, R. Sioshansi, Unit Commitment Under Gas-Supply Uncertainty and Gas-Price Variability, IEEE Trans. Power Syst. 32(3) (2017) 2394-2405. https://doi.org/10.1109/TPWRS.2016.2602659
[23] R. Billinton, R.N. Allan, Reliability Evaluation of Power Systems, Springer, Boston, MA, 1984.
[24] E.S. Pinto, L.M. Serra, A. Lázaro, Evaluation of methods to select representative days for the optimization of polygeneration systems, Renew. Energy 151 (2020) 488-502. https://doi.org/10.1016/j.renene.2019.11.048
[25] T. Schütz, M.H. Schraven, M. Fuchs, P. Remmen, D. Müller, Comparison of clustering algorithms for the selection of typical demand days for energy system synthesis, Renew Energy 129 Part A (2018) 570-582. https://doi.org/10.1016/J.RENENE.2018.06.028
[26] S. Swaminathan, G.S. Pavlak, J. Freihaut, Sizing and dispatch of an islanded microgrid with energy flexible buildings, Appl. Energy 276 (2020) 115355. https://doi.org/10.1016/j.apenergy.2020.115355
[27] U.S. Energy Information Administration. Average frequency and duration of electric distribution outages vary by states. https://www.eia.gov/todayinenergy/detail.php?id=35652, 2018 (Accessed 19 September 2020)
[28] S. Mandal, B.K. Das, N. Hoque, Optimum sizing of a stand-alone hybrid energy system for rural electrification in Bangladesh, J. Clean. Production 200 (2018) 12-27. https://doi.org/10.1016/j.jclepro.2018.07.257
[29] S. Mukherjee, R. Nateghi, M. Hastak, Data on major power outage events in the continental U.S., Data in Brief 19 (2018) 2079-2083. https://doi.org/10.1016/j.dib.2018.06.067
[30] S. Mukherjee, R. Nateghi, M. Hastak, A multi-hazard approach to assess severe weather-induced major power outage risks in the U.S., Reliability Eng. Syst. Saf. 175 (2018) 283-305. https://doi.org/10.1016/j.ress.2018.03.015
[31] Smart Home Dataset with weather Information. % https://www.kaggle.com/taranvee/smart-home-dataset-with-weather-information, 2018 (Accessed 19 September 2020).
[32] I. Alsaidan, A. Khodaei, W. Gao, A Comprehensive Battery Energy Storage Optimal Sizing Model for Microgrid Applications, IEEE Trans. Power Syst. 33(4) (2018) 3968-3980. https://doi.org/10.1109/TPWRS.2017.2769639
[33] Handbook of Battery Energy Storage Systems, Asian Development Bank, Mandaluyong City, Philippines, 2018.
[34] Gurobi - the fastest solver. https://www.gurobi.com/, 2020 (Accessed 8 January 2021)